ОБЪЕДИНЕННЫЙ
ИНСТИТУТ
ЯДЕРНЫХ
ИССЛЕДОВАНИЙ
Дубна

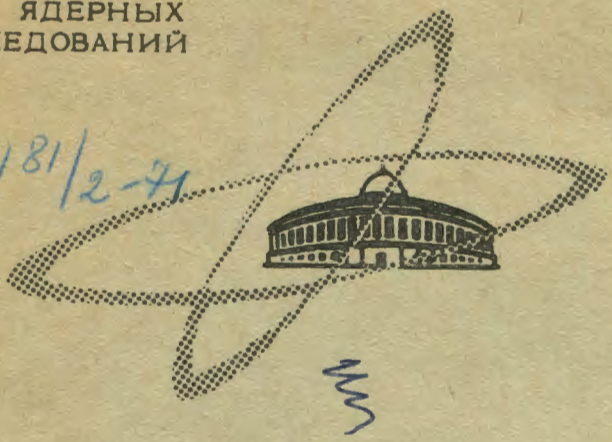

E3–5612

Ludwik Dobrzynski

ON THE POSSIBILITY OF MAGNON INVESTIGATIONS WITHOUT DIRECT ENERGY ANALYSIS USING PULSED NEUTRON SOURCE

1971

Лаборатория нейтронной физики

The diffraction technique in the magnon studies by means of neutron scattering is already known for many years [1]. It was extensively employed in the studies of all magnetic substances: ferro-, antiferro- and ferrimagnets. The purpose of this paper is to propose a version of this technique which could be particularly interesting when combined with a pulsed neutron sourse /PNS/. It will be shown that when magnon dispersion relation is quadratic then the neutron scattering at a given angle is strictly confined to a certain range of incoming and scattered neutron wavelengths. The implication of this fact is that different experimental arrangments may be used for the studies of magnons without energy analysis.

Let $\vec{k}'$ and $\vec{k}$ denote the scattering and primary neutron wavevectors, respectively. Neutrons scattered with magnon creation or magnon annihilation satisfy the momentum and energy conservation laws:

$$\vec{k}' - \vec{k} - 2\pi\vec{\tau} = \vec{q}$$

$$k'^2 - k^2 = \epsilon (E_0 + a q^2) , \qquad (1)$$

where q is the magnon wavevector, E_0 is the energy gap in the magnon dispersion law, $\epsilon = \pm 1$, where the upper sign refers to the magnon annihilation and the lower one to the magnon creation. The geometry of the experiment is shown in Fig. 1. Neutrons impinging at a given angle $(90^\circ - \theta_B)$ in respect to the crystal axis are analyzed along the direction given by the chosen scattering angle ϕ.

Let us write

$$\vec{k}' = \vec{k}'_x + \vec{k}'_z , \qquad (2)$$

where $\vec{k}'_z$ is perpendicular to the scattering plane. With the following abbreviations

$$k_0 = \frac{2\pi\tau}{2\sin\theta_B}$$

$$\frac{|\vec{k}'_x|}{k_0} = x , \quad \frac{|\vec{k}|}{k_0} = y , \quad \frac{|\vec{k}'_z|}{k_0} = z , \quad \frac{E_0}{k_0^2} = a_0 \qquad (3)$$

the solution of eq. (1) in respect to $\vec{q}$ gives the equation of the scattering surface:

$$(1-\epsilon a)x^2 + 2\epsilon a\, xy\cos\phi - \qquad (4)$$

$$- 4\epsilon a\, x \sin\theta_B \sin(\theta_B - \phi) - (1+\epsilon a)y^2 + 4\epsilon a\, y \sin^2\theta_B +$$

$$+ (1-\epsilon a)z^2 - \epsilon [a_0 + 4a \sin^2\theta_B] = 0 .$$

This equation describes an ellipsoid centered at

$$z_0 = 0$$

$$x_0 = 2\epsilon a \sin\theta_B \cdot \frac{\epsilon a \cos\theta_B \sin\phi - \sin(\theta_B - \phi)}{a^2 \sin^2\phi - 1} \qquad (5)$$

$$y_0 = 2\epsilon a \sin\theta_B \cdot \frac{\epsilon a \sin\phi \cos(\theta_B - \phi) - \sin\theta_B}{a^2 \sin^2\phi - 1}$$

if

$$a^2 \sin^2\phi - 1 > 0. \qquad (5a)$$

The ellipsoid is real when

$$\frac{1}{a-\epsilon}\{4a \sin^2\theta_B [1 - \epsilon a \sin(2\theta_B - \phi)\sin\phi] - a_0(a^2 \sin^2\phi - 1)\} > 0 \qquad (6)$$

The vertical cross section of the ellipsoid (4) is a circle with the radius

$$R_z^2 = \frac{4\epsilon a \sin^2\theta_B [1 - \epsilon a \sin(2\theta_B - \phi) \sin\phi]}{(\epsilon a - 1)(a^2 \sin^2\phi - 1)} - \frac{\epsilon a_0}{\epsilon a - 1}. \qquad (7)$$

It is seen that the radius (7) changes continuously with ϕ, and θ_B. This forms the basis of the first experiment which was performed by Riste et al. /2/. In this experiment the angle ϕ was kept constant and the vertical cross section of the ellipsoid was studied for different θ_B. The change of the radius (7) with θ_B leads to the value of a.

It follows from eq. (6) that for given $\phi > 2\theta_B$ one observes the scattering with a magnon annihilation ($\epsilon = +1$) only, while

magnon creation is obtained for $\phi < 2\theta_B$. For example, when $a_0 = 0$ (no energy gap) the condition of occurrence of the unique scattering with magnon annihilation is

$$1 - a \sin(\phi - 2\theta_B) \sin\phi < 0 \tag{8}$$

while

$$1 + a \sin(\phi - 2\theta_B) \sin\phi < 0 \tag{8a}$$

stands for the scattering in which a magnon can only be created.

Some additional restrictions arise from the requirement that x and y must be positive; e.g. in the case of magnon annihilation it leads to the inequality

$$1 < a \cos^2(\phi - 2\theta_B) < a \cos^2\theta_B - 1 \ . \tag{8b}$$

Since the a values are normally of the order of 100, the fulfilment of this condition is not difficult. As an example, Figs 2 and 3 show the scattering surfaces for the annihilation and creation cases, respectively (in the plane of the experiment).

After introducing some further abbreviations;

$$\Delta x = x - x_0 \ , \quad \Delta y = y - y_0 \tag{9a}$$

and

$$\Delta y_0 = \sqrt{\frac{(\epsilon a - 1)^2 R_z}{a^2 \sin^2\phi - 1}} \tag{9b}$$

eq. (4) reduces to the simpler form:

$$(\Delta x - \frac{\epsilon a \cos\phi}{\epsilon a - 1} \Delta y)^2 + \frac{a^2 \sin^2\phi - 1}{(\epsilon a - 1)^2} [(\Delta y)^2 - (\Delta y_0)^2] + z^2 = 0 \tag{10}$$

from which the tangential points (dy/dx = 0) on the scattering surface are the following:

$$x_{1,2} = x_0 \pm \frac{\epsilon a \cos\phi}{\epsilon a - 1} \Delta y_0 \qquad (11)$$

$$y_{1,2} = y_0 \pm \Delta y_0 \ .$$

From these considerations it is seen that the magnon studies without direct energy analysis can be carried out by the following methods:

1. When a steady neutron source is used one may fix the counter and the sample at given positions and change continuously the incoming neutron wavelength. The width of the peak observed will be given by $y_2 - y_1 = 2\Delta y_0$. The same can also be done for the inverted geometry where the sample is exposed to a "white beam" and the scattered neutron wavelength is scanned.

2. In the case when PNS is used the situation becomes more complicated. For any point on the scattering surface the total time of flight (in microseconds) is

$$T = \frac{1588}{|k|} \left(\frac{L_1}{x} + \frac{L_2}{y} \right),$$

where L_1 and L_2 are the neutron flight paths (in meters) from the source to the sample and from the sample to the counter, respectively. Therefore the width of the peak observed, ΔT, is determined by the condition $dT/dx = 0$ (or $dT/dy = 0$) and not $dy/dx = 0$, or $dx/dy = 0$, as in the case of the experiments discussed in the point 1[x].

x) It can be proved that the solutions of the equation $dT/dx = 0$ lie between the solutions of the equations $dy/dx = 0$ and $dx/dy = 0$ which can be found analytically.

The roots of the equation $dT/dx = 0$ must be found numerically for any particular experimental arrangement. The advantages of the experiment with PNS may, however, compensate for this difficulty. These are the following. Because x and y are some functions of the dispersion parameters α and α_0, one sees that in order to find them it is enough to study the change of ΔT as a function of L_1 and L_2. This may be realized for example by means of changing the distance between the sample and the counter. The constant geometry of the experiment is then kept, and this can facilitate the studies of α and α_0 as functions of different external fields. Information on α and α_0 can, in addition, be obtained by studying the magnon width versus scattering angle ϕ or θ_B.

If the resolution of the time-of-flight spectrometer was infinite, then sharp maxima should be observed on the intensity versus time-of-flight curve. These would correspond to the points (x_1, y_1) and (x_2, y_2). The invariably finite resolution will, however, spread out the singularities in the expression for the neutron cross section. In Figs 4 and 5 the widths of the magnon peaks for different sets of θ_B and ϕ are presented. We note that in a certain region of ϕ the peak width increases almost lineary with ϕ for the magnon annihilation case. The slope of this line is approximately inversely proportional to the square root of α.

In Fig. 6 the calculated shapes of the magnon lines are presented for $\theta_B = 8^o$ and $\alpha = 233$, $\alpha_0 = 0$, $L_1 = 13$m, $L_2 = 2.2$ m. In the course of calculations, an infinite resolution of the instrument was assumed. For the same set of parameters, the dependence of the total intensity on $|\phi - 2\theta_B|$ is shown. One can clearly see the following: (a) the shape

of the magnon peak is rather irregular; so the peak half width, which is normally such a convenient parameter, can be not so good experimental parameter to be compared with theory. It can be proposed to use the first and the second moments of the intensity curve in the analysis of the experimental results; (b) the total intensity drops rapidly with $|\phi - 2\theta_B|$ what can be expected from the positions of the scattering surfaces (see Figs 2 and 3). The part of the ellipsoid which lies close to the $y = x$ line gives rise to the neutron scattering on long wavelength magnons. Therefore this part gives the main contribution to the scattered intensity, because of the high population of the magnon states. Because in the case of a magnon creation the accessible range of the magnon wave vectors expands more rapidly than in the annihilation case, the sharper drop of intensity in the former case is not unexpected. On the other hand, even for quite large values of $|\phi - 2\theta_B|$ the main contribution to the intensity comes from the long wavelength magnons. This situation can be convenient in the experimental determination of a distortion of the quadratic dispersion law which should be present e.g. in the case of a dipole-dipole interaction.

Ending this paper, I would like to give my thanks to Dr. A. Holas for much advice in computational problems and to the staff of the Laboratory II of the Institute of Nuclear Research at Swierk for many interesting and stimulating discussions.

References

1. R.J. Elliot, R.D. Lowde. Proc.Roy.Soc., A230, 46 (1955).
2. T. Riste, K. Blinowski, J. Janik. J.Phys.Chem.Sol., 9, 153 (1959).

Received by Publishing Department
on February 8, 1971.

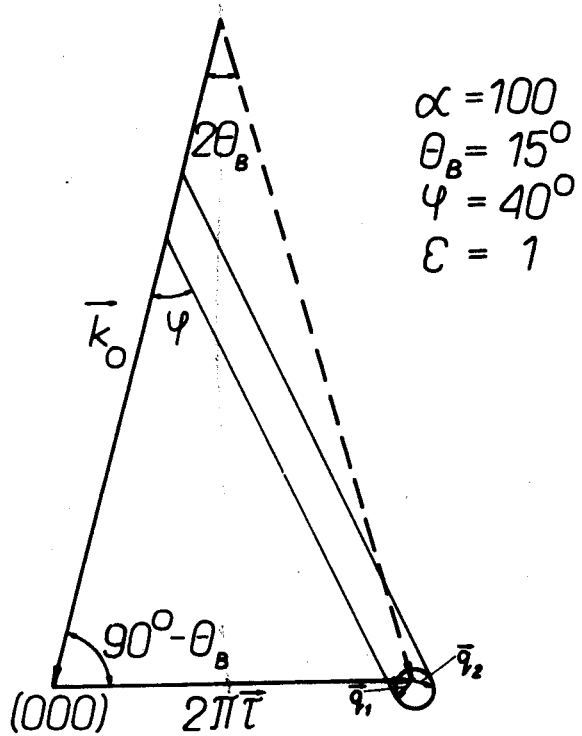

Fig. 1. The geometry of the experiment. The scattering surface is drawn for magnons satisfying the quadratic dispersion relation with $a = 100$, $a_0 = 0$, $\theta_B = 15^\circ$, $\phi = 40^\circ$, $\epsilon = +1$.

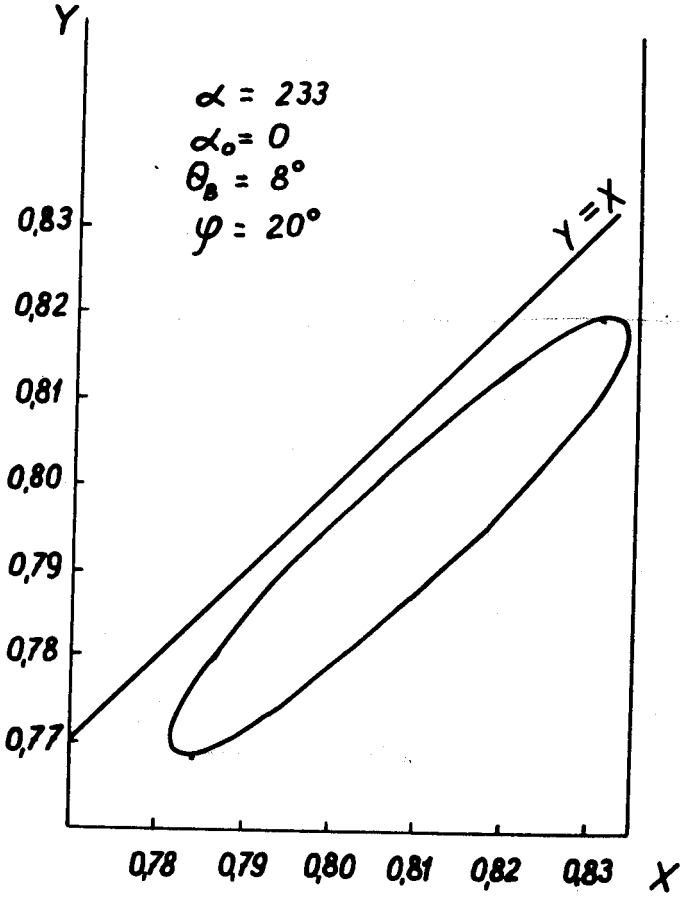

Fig. 2. The scattering surface (in the plane of the experiment) for $\alpha = 233$, $\alpha_0 = 0$, $\theta_B = 8^\circ$ and $\phi = 20^\circ$ (magnon annihilation case).

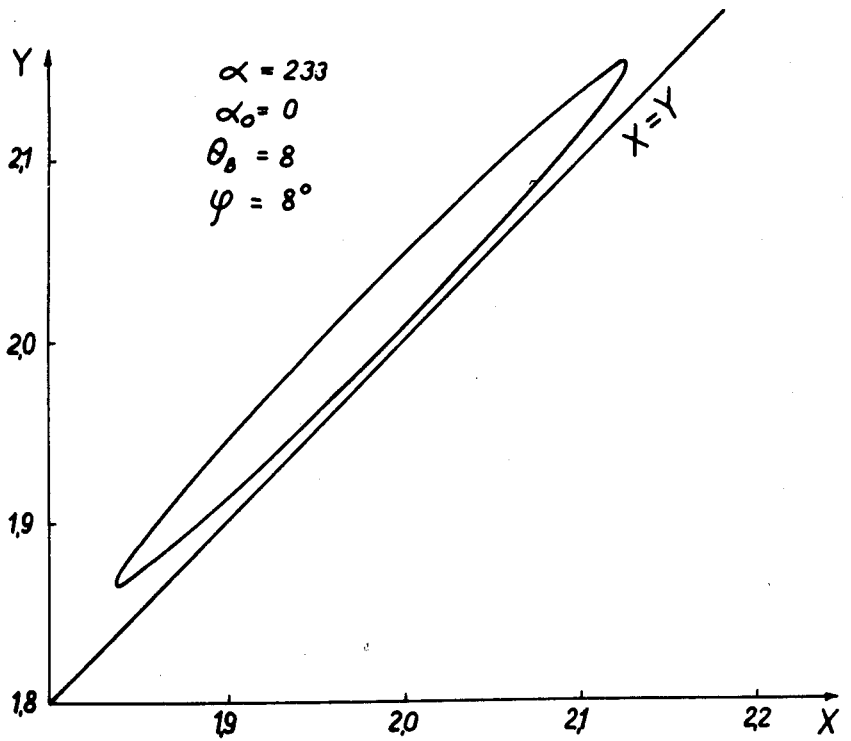

Fig. 3. The scattering surface (in the plane of the experiment) for $a = 233$, $a_0 = 0$, $\theta_B = 8^o$ and $\phi = 8^o$(magnon creation case).

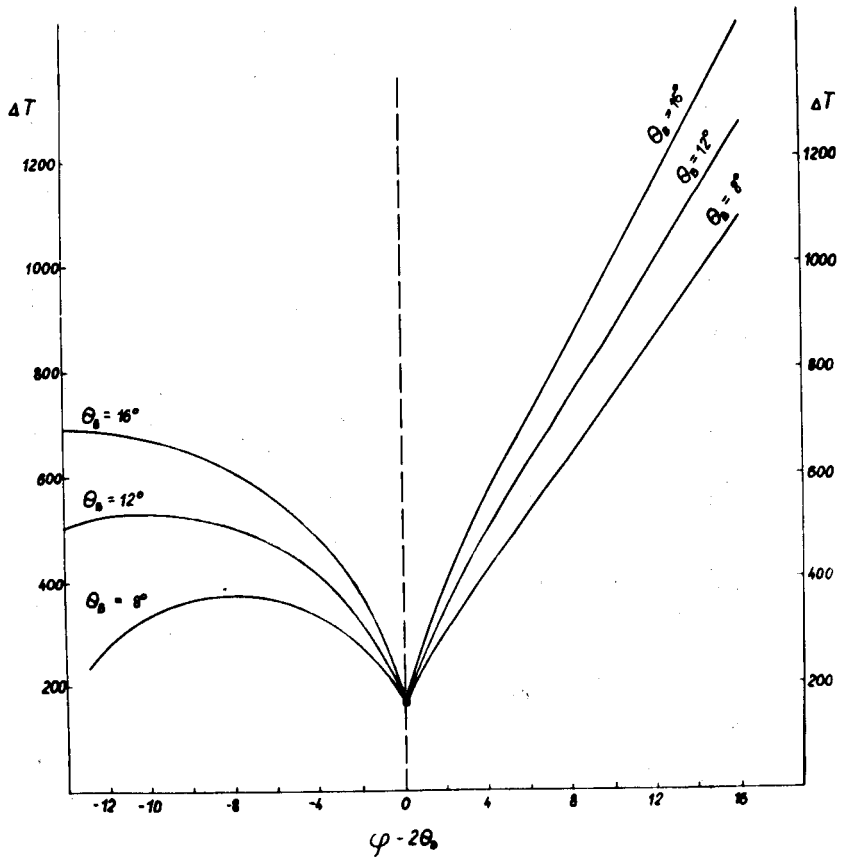

Fig. 4. The dependence of the magnon line width on the scattering angle for various θ_B ; $a = 233$, $a_0 = 0$, $L_1 = 13$m, $L_2 = 2.2$ m.

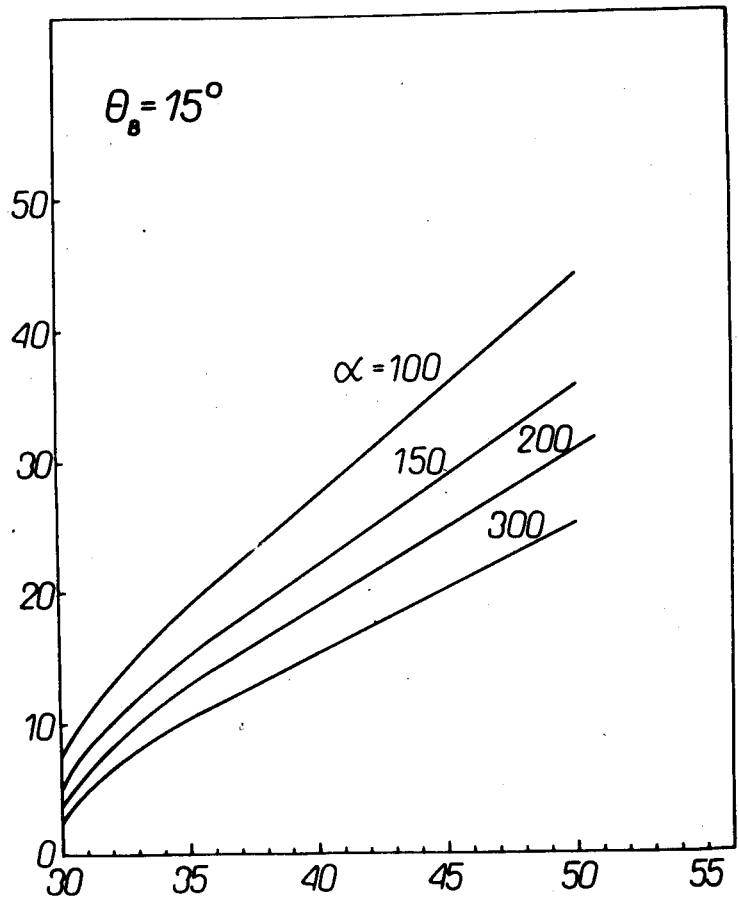

Fig. 5. The dependence of the magnon line width (in arbitrary units) on the scattering angle for various α ; $\theta_B = 15^\circ$, $\alpha_0 = 0$, $L_1 = L_2$.

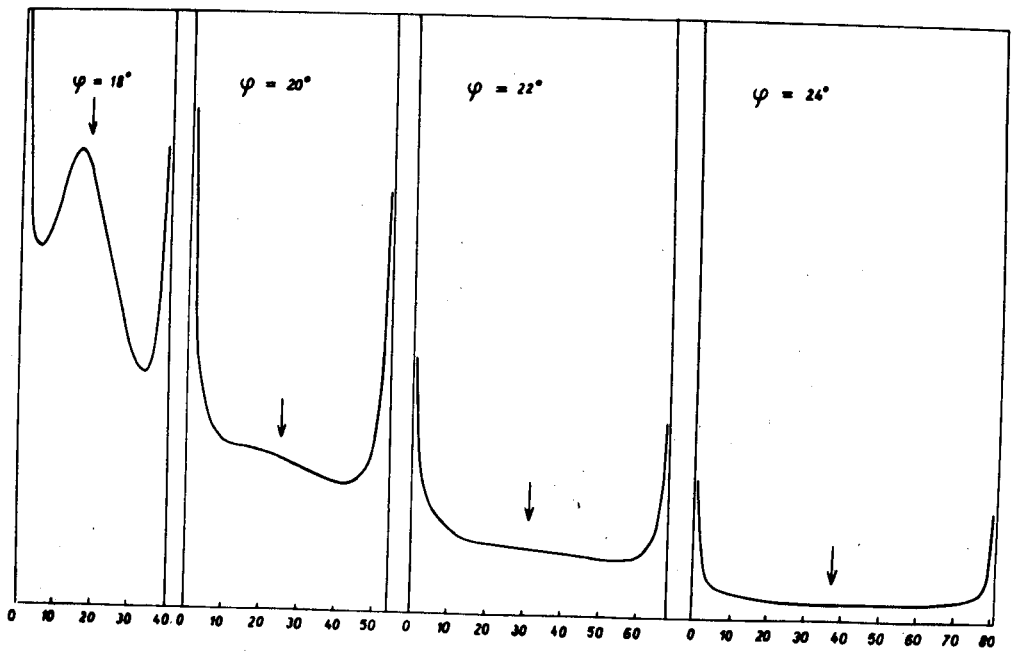

Fig. 6. Intensity distributions (in arbitrary units) for a = 233, a_0 = 0, θ_B = 8°, L_1 = 13m, L_2 = 2,2 m and different ϕ . The right hand side edges of the subsequent peaks (from the left) correspond to the following times of flight: 6000 μ sec, 6728 μ sec, 7455 μsec and 8190 μ sec, respectively; the channel width is 8 sec and the number of channels is shown on the horizontal axis.

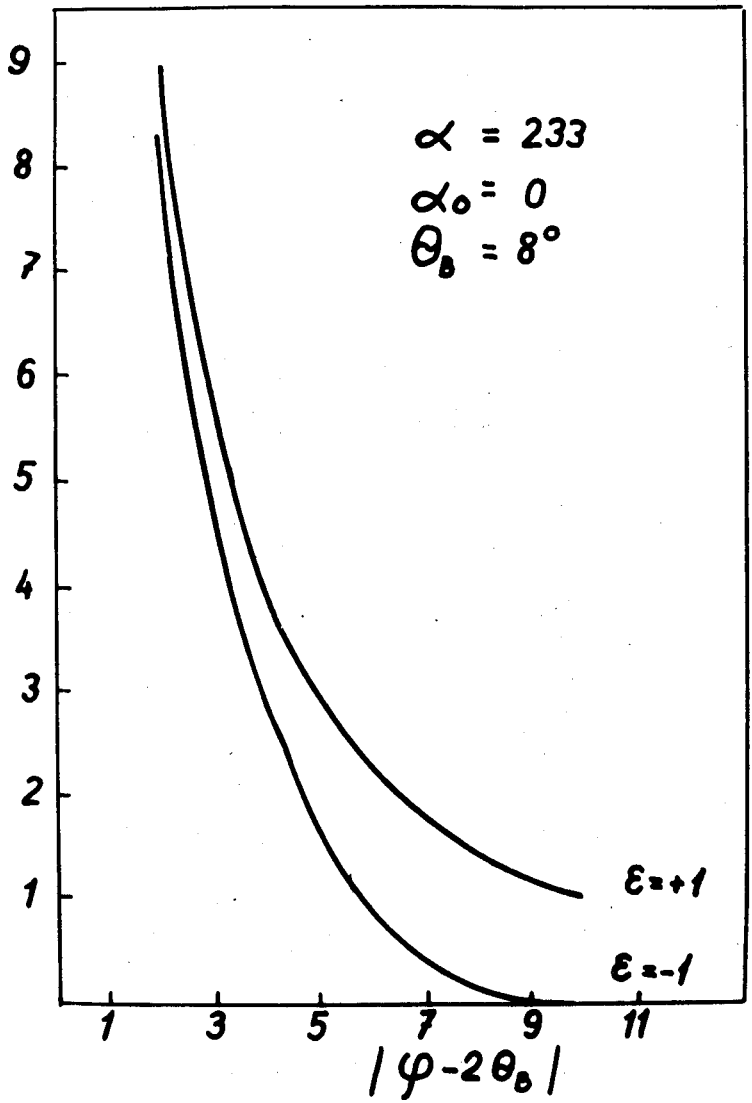

Fig. 7. The total intensity dependence on the $|\phi - 2\theta_B|$ calculated for $\alpha = 233$, $\alpha_0 = 0$, $\theta_B = 8^\circ$.